

FRACTURE TOUGHNESS OF IRRADIATED CANDIDATE MATERIALS FOR ITER FIRST WALL/BLANKET STRUCTURES: SUMMARY REPORT

D. J. Alexander, J. E. Pawel, M. L. Grossbeck, and A. F. Rowcliffe, Oak Ridge National Laboratory, Oak Ridge, TN 37831-6151, and K. Shiba, Japan Atomic Energy Research Institute, Tokai-Mura, Japan

OBJECTIVE

The purpose of this work was to determine the effect of irradiation at low temperatures (less than 300°C) and to damage levels of about 3 dpa on the mechanical properties, in particular the fracture toughness, of candidate materials for ITER first wall/blanket structures.

SUMMARY

Disk compact specimens of candidate materials for first wall/blanket structures in ITER have been irradiated to damage levels of about 3 dpa at nominal irradiation temperatures of either 90 or 250°C. These specimens have been tested over a temperature range from 20 to 250°C to determine J-integral values and tearing moduli. The results show that irradiation at these temperatures reduces the fracture toughness of austenitic stainless steels, but the toughness remains quite high. The toughness decreases as the test temperature increases. Irradiation at 250°C is more damaging than at 90°C, causing larger decreases in the fracture toughness. The ferritic-martensitic steels HT-9 and F82H show significantly greater reductions in fracture toughness than the austenitic stainless steels.

PROGRESS AND STATUS

Introduction

The fracture toughnesses of candidate materials for first wall/blanket structure applications in the International Thermonuclear Experimental Reactor (ITER) have been evaluated at Oak Ridge National Laboratory (ORNL). A variety of austenitic stainless steels have been examined, as well as several additional materials. Specimens were fabricated from material in several different conditions, including annealed or cold worked, as well as weldments. These specimens have been irradiated in the High Flux Isotope Reactor (HFIR) at ORNL. Three capsules were designed, fabricated, and irradiated to dose levels of approximately 3 dpa; this approaches the expected accumulated dose at the end of the Basic Performance Phase of operation of ITER. The helium concentration generated as a result of transmutation of nickel was about 50 appm; this is in the range expected for the ITER first wall blanket and shield structure after a neutron exposure of about 3 dpa. These capsules were designed for irradiation temperatures of either 60 to 125°C (capsules HFIR-JP-18 and -19) or 250 to 300°C (HFIR-JP-17) [1-3]. These temperatures covered the expected range of operating temperatures for stainless steel components in different ITER designs. Some of the results of earlier testing have already been reported [4-6]. This report presents the final results for all of the fracture toughness tests, using the best available tensile data for these final analyses.

Experimental Procedure

Four major alloy types were included in this experiment: American and Japanese type 316 steels (designated US316 and J316, respectively), a European type 316L steel (EC316L), and the JPCA alloy. The compositions of the alloys are given in Table 1. Specimens were in solution annealed (SA), cold-worked (CW), or welded conditions. The J316 material was also tested after a thermomechanical treatment in which it was strained, aged, and recrystallized (SAR). There were a total of 12 variants of the austenitic materials in composition and thermomechanical treatment. The EC316L was welded using 16-8-2 filler metal (see Table 1) and gas tungsten arc (GTA) welding with argon cover gas. Both the plate and the filler wire were provided by Joint Research Centre-Ispra from the European Fusion Stockpile. The JPCA and J316 plate material were supplied by the Japan Atomic Energy Research Institute. The JPCA specimens were welded with filler wire with a composition similar

to the base metal (see Table 1) for both the GTA welding. The US316 material was an air-melted heat from the U.S. fusion program, reference heat X15893. Two ferritic-martensitic steels were also included in this experiment, HT-9 and F82H.

A small disk compact specimen 12.5 mm in diameter was selected for the fracture toughness experiments. The techniques developed for generating the J-integral-resistance (J-R) curve using either unloading compliance (UC) or potential drop (PD) to monitor crack extension are described elsewhere [7-9]. The disk compact specimens [designated DC(T)] were 12.5 mm in diameter by 4.63 mm thick. All specimens were fabricated from the middle of the thickness of the parent plates of material, with the notch oriented so that crack growth would occur parallel to the rolling direction (T-L orientation). The specimens were fatigue precracked at room temperature to a crack length to specimen width ratio (a/W) of roughly 0.5 and then side grooved 10% of their thickness on each side, prior to irradiation.

Tests were conducted in general accordance with American Society for Testing and Materials standards E 813-89, Standard Test Method for J_{Ic} , A Measure of Fracture Toughness, and E 1152-87, Standard Test Method for Determining J-R Curves. The equations in E 1152-87 were used for the J calculations. The specimens were tested with a computer-controlled testing and data acquisition system. Tests in the laboratory used an 89-kN capacity servohydraulic test machine. In the hot cell, a 445-kN capacity servohydraulic testing machine with an 22-kN load cell was used. All tests were run in strain control. The displacements were measured with an "outboard" clip gage that seated in grooves machined on the outer edge of the specimen along the load line [7,8]. This arrangement provided very good load-displacement data and so the UC technique was used for all tests. Test temperatures from 90 to 250°C were maintained within $\pm 2^\circ\text{C}$ of the desired temperature with a split-box furnace that enclosed the specimen and the grips during the test. Temperature was monitored throughout the testing with a thermocouple that was held in contact with the specimen by a spring-loaded clip. Tensile data from specimens included in the capsules were used for calculations in the J-R analyses [10]. Estimated values were taken from literature data when necessary.

After testing, the specimens were heat tinted to mark the crack extension. The initial and final crack lengths for the unirradiated specimens were measured with an optical measuring microscope. For the irradiated specimens, photographs of the fracture surfaces were fastened to a digitizing tablet to measure the crack lengths.

Materials with very high toughness and low yield strength, such as the annealed austenitic stainless steels, proved to be more difficult to test than material with lower toughness such as HT-9. The soft, tough materials showed enormous crack-tip blunting before stable crack growth began. This resulted in gross changes in the specimen geometry, and so the crack length predictions were not very accurate. The J-R curve was much steeper than the calculated blunting line. In these cases, the data were used to calculate a blunting line. A straight line was fit by eye through the initial portion of the data points, and a second line was drawn parallel to the first but offset by an amount corresponding to a crack extension of 0.2 mm following ASTM E 813-89. The candidate toughness value J_Q was then determined from the intersection of the data with this offset line. In cases where the data rose very steeply, the test was terminated before there was enough crack growth to cross the second exclusion line (drawn corresponding to a crack extension of 1.5 mm as defined in the ASTM E 813-89). As a result, no tearing modulus value could be calculated. Materials with lower toughness, such as the cold-worked austenitic stainless steels, behaved in a much more conventional manner. For these materials, the data followed the calculated blunting line quite closely, so no additional construction was required. These specimens also showed very good agreement between the measured and predicted final crack lengths.

Results and Discussion

The results of the testing are given in Tables 2 to 6. These tables also includes the tensile values used in the analyses. The tensile data for the specimens included in these experiments are given in Table 7. The toughness of the austenitic steels is very high. In general, the toughness decreases as the test temperature increases, but remains very high. An extended discussion of these results and a comparison to literature data is presented elsewhere [6].

Both before and after irradiation, the fracture toughnesses of the solution annealed materials are very high ($K_{Ic} > 150 \text{ MPa}\sqrt{\text{m}}$) in the test temperature range. The toughness decreases slightly as the temperature increases, but remains very high, even after irradiation and testing at 250°C . Irradiation at 250°C causes a greater decrease in the toughness than irradiation at 90°C . The range of fracture toughness values of these materials is in the upper range of previously reported data from a variety of steels, reactor environments, and test methods [11-16]. The fracture toughness of the cold-worked material is generally lower than that of the annealed material, typically by about 75 to $100 \text{ MPa}\sqrt{\text{m}}$, both before and after irradiation.

The fracture toughness of the ferritic materials are also reduced by these irradiations. The F82H alloy is more resistant to damage than the HT-9 material. Both of these alloys show high toughness at high test temperatures (250°C) with lower toughness at 25°C (Table 6). The HT-9 specimen irradiated at 250°C fractured in a brittle manner when tested at room temperature. The load-displacement trace was linear, and the value of the fracture toughness ($31 \text{ MPa}\sqrt{\text{m}}$) is so low that it satisfies the specimen thickness validity criteria for plane strain fracture toughness, despite the very small specimen size. The F82H specimen irradiated at 250°C and tested at 25°C also shows a lower toughness than when tested at 250°C , but the load-displacement curve showed considerable nonlinearity and the final fracture, although unstable, occurred at a high toughness level of $156 \text{ MPa}\sqrt{\text{m}}$.

There is surprisingly little data for comparison with these results. These stainless steel alloys are very tough, and so the fracture toughness is not usually a concern. Odette and Lucas [11,12], Tavassoli [13], and Boutard [14] have recently surveyed the available data for the effects of low temperature irradiation ($< 400^\circ\text{C}$) on the mechanical properties, including the fracture toughness, of austenitic stainless steels. There is very little data that is directly comparable to the present work, but the overall trend of the data shows that irradiation reduces the fracture toughness, but that it still remains high, in agreement with the present results.

A trend line of toughness vs irradiation dose for austenitic stainless steels is shown in Fig. 1, adapted from the review article by Lucas [15]. This represents data for a variety of wrought materials irradiated at temperatures from 290 to 430°C . After a rapid initial decrease, the minimum toughness values (note that K values are shown) approach $50 \text{ MPa}\sqrt{\text{m}}$ for doses beyond 10 dpa . Also shown are data from Sindelar et al. [16] for a 1950s vintage type 304 stainless steel irradiated at 100 to 155°C to doses up to 2 dpa . The data from the present work fall into two groups. Results from the higher irradiation temperature (250 to 300°C) are consistent with the published data represented by the trend line which indicates toughness values in the range of 200 to $250 \text{ MPa}\sqrt{\text{m}}$ for doses up to 3 dpa . For the lower irradiation temperature (60 to 125°C) the reduction in fracture toughness is significantly less with the data falling well above the trend line. This is likely the result of a different microstructural response to irradiation, and a reduced level of irradiation hardening for the same dose as compared to higher temperature irradiation. The data of Sindelar et al. [21] fall well below the present data for low temperature irradiation, likely reflecting the greater sensitivity to irradiation damage of the 1950s vintage weldments of type 304 stainless steel.

It should be noted that most of the J-R data generated with this small disk compact specimen do not satisfy all of the validity requirements of the ASTM standards, and so these data are not valid. ASTM standard E 1152-87, "Standard Test Method for Determining J-R Curves," sets three limits based on the specimen size. The maximum J-integral measurement capacity is given by the smaller of

$$J_{\max} = b \sigma_f / 20 \quad \text{or} \quad (1)$$

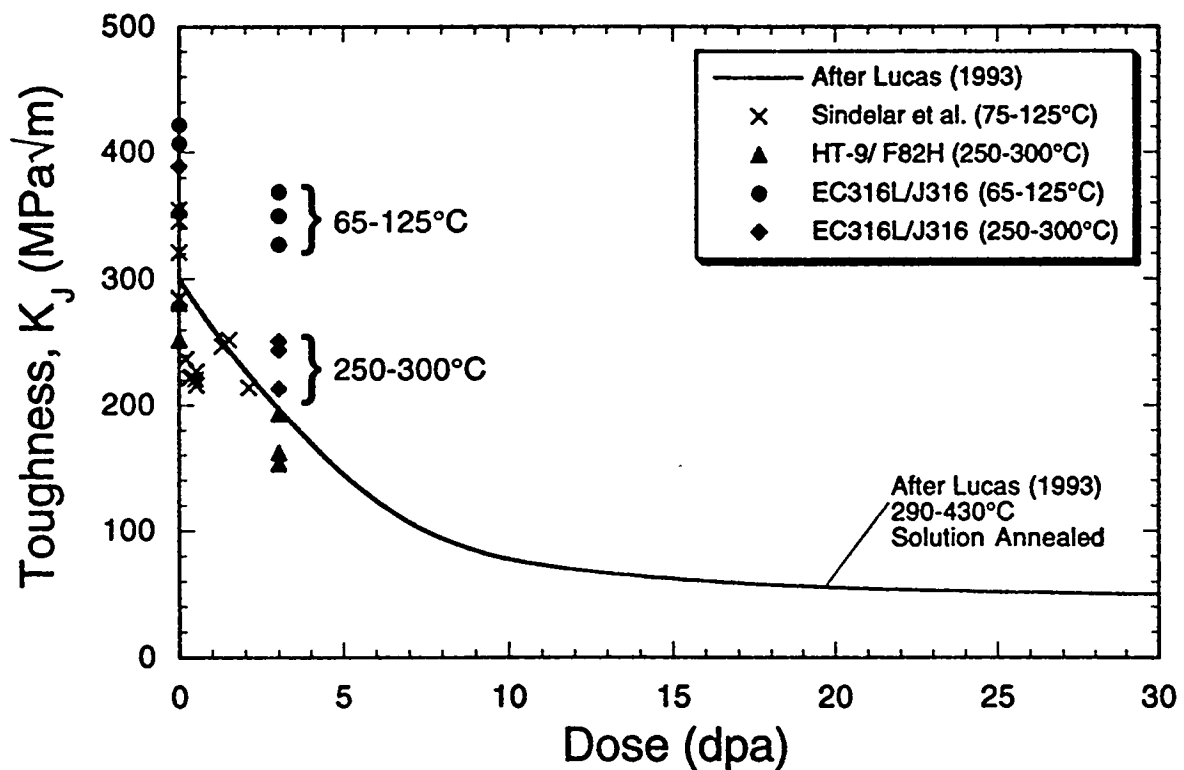
$$J_{\max} = B \sigma_f / 20, \quad (2)$$

where

- b = initial ligament size,
 B = specimen thickness, and
 σ_f = flow stress (average of yield and ultimate tensile stresses).

If the crack length to specimen width ratio (a/W) is 0.5, these are identical, as b will equal B for this specimen, in this case. For nearly all of the data, the measured J-integral values greatly exceed this limit. Only the lowest toughness materials have J-integral values low enough to satisfy these conditions. However, there is another even more limiting condition. The maximum allowable crack extension is limited to $0.1b$. For an initial a/W value of 0.5, which was intended, the resultant maximum allowable crack extension is only 0.46 mm, well short of the second exclusion line at 1.5 mm of crack extension. If the initial crack length is longer, as was nearly always the case, even less crack extension is allowed. For tough materials, the limit for crack extension will be reached when the J-R curve data are still on the blunting line, and stable tearing has not even begun to occur. Even for lower toughness conditions, only a few of the data points will be valid, and the bulk of the J-R curve is beyond the limit of validity. The values given in Tables 2 to 6 have been generated by using all the data between the first and second exclusion lines to determine the curve fit for calculation of J_Q , even though this data are not valid according to ASTM E 1152-87.

It must be emphasized that the J-R data, despite being invalid according to ASTM E 1152, are not incorrect. The size limitations imposed are conservative, and the J-integral values are quite likely still true measures of the materials' toughness, as long as the limits are not exceeded by too great a margin. The J-R curves are directly applicable to structures of the same thickness as the specimens.



The J-R curves are of great value in elucidating the materials' responses to irradiation. The J-R curves show how these materials are embrittled by irradiation as a function of irradiation temperature and damage level. They also show which materials are most resistant to embrittlement, and give an indication of the rate at which embrittlement will occur for the present irradiation and material conditions. These are very useful pieces of information for evaluating candidate structural materials for ITER applications.

CONCLUSIONS

Specimens of several austenitic stainless steels and two ferritic-martensitic steels have been irradiated in HFIR to about 3 dpa at nominal irradiation temperatures of 90 or 250°C. For the austenitic stainless steels, irradiation reduces the fracture toughness, and irradiation at 250°C is more damaging than irradiation at 90°C. The fracture toughness decreases with increasing test temperature, for all the austenitic materials. The annealed materials have higher toughnesses than the cold-worked materials. The toughness of the cold-worked materials is still high, with the exception of the US316 material. The welds also have high toughnesses. For the ferritic-martensitic materials, the specimens irradiated at 250°C and tested at room temperature fail in an unstable manner. The F82H has a higher toughness than the HT-9 alloy.

ACKNOWLEDGMENTS

The fracture toughness testing was performed by R. L. Swain. The manuscript was prepared by J. L. Bishop.

REFERENCES

1. A. W. Longest, D. W. Heatherly, K. R. Thoms, and J. E. Corum, "Design and Fabrication of HFIR-MFE-JP Target Irradiation Capsules," *Fusion Reactor Materials Semiannual Progress Report for Period Ending March 31, 1991*, DOE/ER-0313/10, 1991, p. 3.
2. A. W. Longest, D. W. Heatherly, J. E. Wolfe, K. R. Thoms, and J. E. Corum, "Fabrication and Irradiation of HFIR-MFE-JP-17, -18, and -19 Target Irradiation Capsules," *Fusion Reactor Materials Semiannual Progress Report for Period Ending September 30, 1991*, DOE/ER-0313/11, 1992, p. 30.
3. A. W. Longest, D. W. Heatherly, K. R. Thoms, and J. E. Corum, "Fabrication and Irradiation of HFIR-MFE-JP-17, -18, and -19 Target Irradiation Capsules," *Fusion Reactor Materials Semiannual Progress Report for Period Ending March 31, 1992*, DOE/ER-0313/12, 1992, p. 24.
4. D. J. Alexander, J. E. Pawel, M. L. Grossbeck, and A. F. Rowcliffe, "Fracture Toughness of Irradiated Candidate Materials for ITER First Wall/Blanket Structures: Preliminary Results," *Fusion Reactor Materials Semiannual Progress Report for Period Ending March 31, 1992*, DOE/ER-0313/14, 1993, p. 277.
5. J. E. Pawel, D. J. Alexander, M. L. Grossbeck, A. W. Longest, A. F. Rowcliffe, G. E. Lucas, S. Jitsukawa, A. Hishinuma, and K. Shiba, "Fracture Toughness of Candidate Materials for ITER First Wall, Blanket, and Shield Structures," *Fusion Reactor Materials Semiannual Progress Report for Period Ending September 30, 1993*, DOE/ER-0313/15, 1992, p. 173.
6. D. J. Alexander, J. E. Pawel, M. L. Grossbeck, A. F. Rowcliffe, and K. Shiba, "Fracture Toughness of Irradiated Candidate Materials for ITER First Wall/Blanket Structures," *Effects of Radiation on Materials: 17th Volume, ASTM STP 1270*, D. S. Gelles, R. K. Nanstad, A. S. Kumar, and E. A. Little, Editors, American Society for Testing and Materials, Philadelphia, 1996, in press.
7. D. J. Alexander, "Fracture Toughness Measurements with Subsize Disk Compact Specimens," *Fusion Reactor Materials Semiannual Progress Report for Period Ending March 31, 1992*, DOE/ER-0313/12, 1992, p. 35.

8. D. J. Alexander, "Fracture Toughness Measurements with Subsize Disk Compact Specimens," in *Small Specimen Test Techniques Applied to Nuclear Reactor Vessel Thermal Annealing and Plant Life Extension*, ASTM STP 1204, W. R. Corwin, F. M. Haggag, and W. L. Server, Editors, American Society for Testing and Materials, Philadelphia, 1993, p. 130.
9. C. Elliot, M. Enmark, G. E. Lucas, and G. R. Odette, "Development of Disc Compact Specimens and Test Techniques for HFIR Irradiations," *Fusion Reactor Materials Semiannual Progress Report for Period Ending September 30, 1990*, DOE/ER-0313/9, 1991, p. 7.
10. J. E. Pawel, unpublished research, Oak Ridge National Laboratory, 1994.
11. G. R. Odette and G. E. Lucas, *J. Nucl. Mater.*, Vol. 179-181, 1991, p. 572.
12. G. R. Odette and G. E. Lucas, *J. Nucl. Mater.*, Vol. 191-194, 1992, p. 50.
13. A. A. Tavassoli, "Assessment of Austenitic Stainless Steels," N.T. SRMA 94-2061, F.A. 3591-ITER, CEA, CEN-Saclay, 91191 Gif Sur Yvette, France, June 1994.
14. J. L. Boutard, *J. Nucl. Mater.*, Vol. 179-81, 1991, p. 1179.
15. G. E. Lucas, *J. Nucl. Mater.*, Vol. 206, 1993, p. 287.
16. R. L. Sindelar, G. R. Caskey, J. K. Thomas, J. R. Hawthorne, A. L. Hiser, R. A. Lott, J. A. Begley, and R. P. Shogan, "Mechanical Properties of 195's Vintage Type 304 Stainless Steel Weldment Components, After Low Temperature Irradiation," in *Effects of Radiation on Materials: 16th International Symposium*, ASTM STP 1175, A. S. Kumar, D. S. Gelles, R. K. Nanstad, and E. A. Little, Editors, American Society for Testing and Materials, Philadelphia, 1993, p. 714.

Table 1. Specimen alloy compositions and processing

Alloy	Composition (wt %)											
	Fe	Ni	Cr	Ti	Mo	Mn	Si	C	N	V	W	Ta
JPCA	Bal	15.95	14.3	0.21	2.4	1.6	0.54	0.064	0.003	--	--	--
US316	Bal	12.4	17.3	--	2.1	1.7	0.67	0.061	--	--	--	--
EC316L	Bal	12.3	17.4	--	2.3	1.8	0.46	0.024	0.06	--	--	--
J316	Bal	13.95	16.77	--	2.31	0.23	0.04	0.038	0.011	--	--	--
16-8-2 weld wire	Bal	8.98	16.28	--	2.16	1.82	0.060	0.036	0.029	--	--	--
JPCA weld wire	Bal	16.06	14.39	0.23	2.44	1.77	0.35	0.057	0.0095	--	--	--
HT-9	Bal	0.51	12.1	--	1.04	0.57	0.17	0.20	0.027	0.28	0.45	--
F82H	Bal	0.05	7.65	--	--	0.49	0.09	0.093	0.0018	0.18	1.98	0.038

JPCA Annealed: Solution annealed (1120°C/1 h/water quench).
 JPCA Cold Worked: Annealed + cold worked 20%.
 J316 Annealed: Solution annealed (1060°C/15 min/water quench).
 J316 Cold Worked: Annealed + cold worked 20%.
 J316 Strained, Aged, Recrystallized: 1150°C/1 h + 60% cold work + 650°C/15 h + 800°C/15 h.
 EC316L Annealed: Solution annealed.
 US316 Annealed: Cold worked 50% + annealed (1050°C/1 h).
 US316 Cold Worked: Annealed + 20% cold work.
 HT-9: 1050°C/1 h/air cooled + 780°C/2.5 h/air cooled.
 F82H: 1040°C/0.5 h + 740°C/1.5 h/air cooled.

Table 2. Fracture toughness and tensile properties of EC316L

Material	Specimen	Irradiation temperature (°C)	Test temperature (°C)	J_Q (kJ/m ²)	K_I^a (MPa√m)	T	σ_y (MPa)	σ_u (MPa)	E (GPa)
EC316L Annealed	FA14	Unirradiated	22	847	404	NA	296 ^b	579	193
	FA22	Unirradiated	100	889	407	NA	283 ^b	517	186
	FA5	Unirradiated	200	697	353	NA	214 ^b	448	179
EC316L Annealed	FA16	90	25	781	388	107	625	700	193
	FA3	90	25	800	393	93	625	700	193
	FA21	90	25	634	350	135	625	700	193
	FA6	90	100	671	353	129	607 ^b	676	186
	FA11	90	100	574	327	92	607 ^b	676	186
	FA17	90	200	548	314	221	525	600	179
	FA2	250	25	417	284	39	850	860	193
EC316L Annealed	FA10	250	100	387	268	38	800	810	186
	FA9	250	250	257	214	47	741 ^b	748	179
	FA18	250	250	353	252	42	741 ^b	748	179
EC316L PERP ^c	Unirradiated	90	831	393	NA	283	517	186	
EC316L PERP ^c	90	90	512	309	102	607	676	186	
EC316L Weld	FB3	Unirradiated	22	772	386	NA	310 ^b	614	193
	FB14	Unirradiated	90	710	363	NA	221 ^b	476	186
	FB17	Unirradiated	250	610	331	NA	241 ^b	448	179
EC316L Weld	FB4	90	341	252	109	627 ^b	703	186	
EC316L Weld	FB5	250	250	160	170	29	741	748	179
	FB13	250	250	152	165	23	741	748	179

^a $K_I^2 = J_Q E$.^bData from tensile test from these experiments.^cPERP = Specimens oriented so that crack growth was perpendicular to the rolling direction.

Table 3. Fracture toughness and tensile properties of J316

Material	Specimen	Irradiation temperature (°C)	Test temperature (°C)	J_0 (kJ/m ²)	K_{Ic}^a (MPa√m)	T	σ_y (MPa)	σ_u (MPa)	E (GPa)
J316 Annealed	FC8	Unirradiated	22	790	391	NA	100	450	193
	FC24	Unirradiated	90	959	423	NA	90 ^b	427	186
	FC21	Unirradiated	250	843	388	NA	62 ^b	372	179
J316 Annealed	FC12	90	90	737	370	100	689 ^b	696	186
	FC16	90	250	620	333	99	600	625	179
J316 Annealed	FC10	250	90	453	291	59	825	850	186
	FC2	250	250	333	244	55	750	775	179
J316 SAR ^c	FM5	Unirradiated	22	595	339	103	525	650	193
	FM8	Unirradiated	90	548	319	63	517 ^b	634	186
	FM9	Unirradiated	250	392	265	107	455	559	179
J316 SAR ^c	FM11	90	90	263	221	36	690	696	186
J316 SAR ^c	FM2	250	250	170	175	28	750	775	179
J316 CW ^d	FD7	Unirradiated	22	870	410	71	717 ^b	765	193
	FD5	Unirradiated	90	591	332	101	593 ^b	641	186
	FD1	Unirradiated	250	328	243	89	572 ^b	607	179
J316 CW ^d	FD12	90	90	479	299	46	827 ^b	841	186
	FD8	90	250	302	233	40	725	750	179
J316 CW ^d	FD10	250	90	271	225	40	889 ^b	938	186
	FD11	250	250	138	157	18	821 ^b	827	179

^a $K_{Ic}^2 = J_0 E$.^bData from tensile test from this experiment.^cSAR = Strained, aged, and recrystallized.^dCW = Cold worked 20%.

Table 4. Fracture toughness and tensile properties of JPCA

Material	Specimen	Irradiation temperature (°C)	Test temperature (°C)	J_0 (kJ/m ²)	$K_{J_0}^2$ (MPa√m)	T	σ_y (MPa)	σ_u (MPa)	E (GPa)
JPCA Annealed	FF10	Unirradiated	22	616	345	NA	331 ^b	600	193
	FF13	Unirradiated	100	706	363	158	269 ^b	510	186
	FF20	Unirradiated	200	498	299	82	269 ^b	483	179
JPCA Annealed	FF6	90	25	349	260	23	750	770	193
	FF5	90	25	355	262	41	750	770	193
	FF16	90	100	310	240	34	717 ^b	738	186
	FF15	90	100	312	241	31	717 ^b	738	186
	FF2	90	200	225	201	46	614 ^b	634	179
JPCA Annealed	FF3	250	25	271	229	18	900	950	193
	FF11	250	100	133	157	13	862 ^b	910	186
	FF18	250	250	123	148	14	779 ^b	827	179
JPCA EBW ^e	FR7	Unirradiated	250	619	333	NA	269	483	179
JPCA EBW ^e	FR11	90	90	885	406	101	717	738	186
	FR12	250	250	315	238	52	779	827	179
JPCA CW ^d	FE6	Unirradiated	22	365	266	45	625	650	193
	FE3	Unirradiated	90	306	239	55	600 ^b	627	186
	FE1	Unirradiated	250	181	180	82	524 ^b	572	179
JPCA CW ^d	FE8	90	90	167	176	24	931 ^b	952	186
JPCA CW ^d	FE7	250	250	124	149	8	868 ^b	896	179
	FG10	Unirradiated	22	655	356	NA	331	600	193
JPCA Weld	FG13	Unirradiated	90	1020	436	NA	269	510	186
	FG1	Unirradiated	250	959	415	NA	269	483	179
JPCA Weld	FG8	90	90	316	242	46	717	738	186
JPCA Weld	FG12	250	250	234	205	27	779	827	179

* $K_{J_0}^2 = J_0 E$.^bData from tensile test from these experiments.^eEBW = Electron beam weld.^dCW = Cold worked 20%.

Table 5. Fracture toughness and tensile properties of US316

Material	Specimen	Irradiation temperature (°C)	Test temperature (°C)	J_Q (kJ/m ²)	K_I^* (MPa√m)	T	σ_y (MPa)	σ_u (MPa)	E (GPa)
US316 Annealed	FK16	Unirradiated	22	234	213	79	262 ^b	607	193
	FK6	Unirradiated	90	235	209	76	186 ^b	510	186
	FK8	Unirradiated	250	213	195	88	152 ^b	462	179
US316 Annealed	FK7	90	90	156	171	17	500	550	186
US316 Annealed	FK10	250	250	36	80	6	650	700	179
US316 CW ^c	FL13	Unirradiated	22	35	82	4	683 ^b	793	193
	FL8	Unirradiated	90	34	80	0	662 ^b	724	186
	FL9	Unirradiated	250	28	71	-	572 ^b	648	179
US316 CW ^c	FL15	90	90	22	64	0	848 ^b	862	186
US316 CW ^c	FL5	250	250	15	52	0	825	850	179

* $K_I^2 = J_Q E$.
^bData from tensile test from these experiments.
^cCW = Cold worked 20%.

Table 6. Fracture toughness and tensile properties of ferritic-martensitic alloys

Material	Specimen	Irradiation temperature (°C)	Test temperature (°C)	J_Q (kJ/m ²)	K_I^* (MPa√m)	T	σ_y (MPa)	σ_u (MPa)	E (GPa)
HT-9	FH11	Unirradiated	22	484	316	104	476 ^b	696	207
	FH3	Unirradiated	90	470	307	91	414 ^b	621	200
	FH4	Unirradiated	250	415	283	131	427 ^b	627	193
HT-9	FH1	90	90	283	238	41	903 ^b	917	200
HT-9	FH5	250	25	5	31	-	950	1000	207
	FH6	250	250	140	164	17	876 ^b	931	193
F82H	F13	Unirradiated	250	334	254	122	448 ^b	531	193
F82H	F14	250	25	117	156	-	950	975	207
	F11	250	250	197	195	22	855 ^b	855	193

* $K_I^2 = J_Q E$.
^bData from tensile specimen from these experiments.

Table 7. Tensile Properties of Irradiated and Unirradiated Materials.

Alloy	Specimen I.D.	Dose (dpa)	Helium (appm)	Irrad. Temp (°C)	Test Temp. (°C)	YS (MPa)	UTS (MPa)	E ₁ (%)	E _t (%)	Strain to Necking (%)	
JPCA	FF4T	0	0	-	25	331	600	48.8	60.3	51.5	
SA	FF3T	0	0	-	90	269	510	40.8	50.2	41.8	
	FF6T	0	0	-	250	269	483	32.8	40.1	33.2	
	FF7T	2.9	64	83-101	90	717	738	19.3	32.3	23.3	
	FF9T	2.9	64	83-101	250	614	634	15.7	22.7	16.7	
	FF2T	2.9	69	250-300	250	779	827	2.8	11.8	3.0	
	FF5T	2.9	69	250-300	90	862	910	4.9	17.2	7.3	
	JPCA	FE16T	0	0	-	90	600	627	3.0	17.1	4.4
CW	FE15T	0	0	-	250	524	572	2.5	13.6	3.2	
	FE17T	2.9	64	83-101	90	931	952	0.8	10.5	0.9	
	FE18T	2.9	69	250-300	250	869	896	1.5	10.9	2.1	
	FE19T	2.9	69	250-300	90	979	1020	2.5	15.7	3.3	
	J316	FC27	0	0	-	90	90	427	69.3	83.5	73.7
SA	FC30	0	0	-	250	62	372	51.6	62.4	53.3	
	FC28	2.9	64	83-101	90	690	696	0.3	38.7	29.0	
J316	FD2T	0	0	-	25	717	765	2.7	21.0	6.6	
CW	FD7T	0	0	-	90	593	641	4.7	23.5	11.0	
	FD1T	0	0	-	250	572	607	1.5	16.2	1.8	
	FD6T	2.9	64	83-101	90	827	841	0.5	15.7	0.5	
	FD3T	2.9	69	250-300	250	821	827	0.3	10.5	0.3	
	FD5T	2.9	69	250-300	90	889	938	1.2	13.7	1.4	
	EU316L	FA27T	0	0	-	25	298	582	59.3	68.5	62.0
SA	FA21T	0	0	-	90	285	516	48.3	57.2	50.2	
	FA26T	0	0	-	250	214	451	39.5	51.3	40.8	
	FA23T	2.9	64	83-101	90	610	674	34.7	45.0	37.7	
	FA24T	2.9	64	83-101	90	605	677	34.7	46.1	37.0	
	FA22T	2.9	69	250-300	250	760	764	0.4	18.8	11.7	
	FA25T	2.9	69	250-300	250	724	735	0.6	20.8	12.7	
	EU316L	FB18T	0	0	-	25	308	616	49.6	56.3	50.6
WELD	FB17T	0	0	-	90	224	473	38.3	44.8	39.0	
	FB22T	0	0	-	250	242	449	26.5	39.3	27.9	
	FB19T	2.9	64	83-101	90	625	707	18.8	26.1	20.3	
	HT-9	FH6T	0	0	-	25	473	695	14.3	24.1	14.3
FH5T	FH5T	0	0	-	90	416	622	14.1	23.7	14.1	
	FH4T	0	0	-	250	425	624	12.1	20.8	12.1	
	FH1T	2.9	2	83-101	90	903	914	0.4	8.7	0.4	
	FH2T	2.9	2	250-300	250	875	932	6.2	13.4	6.2	
	F82H	FI19	0	0	-	25	573	682	5.4	15.5	5.4
	FI18	FI18	0	0	-	90	571	660	4.5	15.3	4.5
FI17		0	0	-	250	507	577	3.2	13.3	3.2	
FI16		0	0	-	250	451	530	3.4	13.3	3.4	
FI13		2.9	30	250-300	250	852	856	0.3	7.8	0.3	
FI14		2.9	30	250-300	90	723	821	8.2	17.7	8.2	